Princeton Plasma Physics Laboratory

PPPL- 4546

PPPL- 4546

Modular Coils and Plasma Configurations for Quasi-axisymmetric Stellarators

L.P. Ku and A.H. Boozer

September, 2010

Prepared for the U.S. Department of Energy under Contract DE-AC02-09CH11466.

Princeton Plasma Physics Laboratory
Report Disclaimers

Full Legal Disclaimer

Trademark Disclaimer

PPPL Report Availability

Princeton Plasma Physics Laboratory:

http://www.pppl.gov/techreports.cfm

Office of Scientific and Technical Information (OSTI):

http://www.osti.gov/bridge

Related Links:

U.S. Department of Energy

Office of Scientific and Technical Information

Fusion Links

Modular coils and plasma configurations for quasi-axisymmetric stellarators

L. P. Ku[1] and A. H. Boozer[2]
[1]Princeton Plasma Physics Laboratory, Princeton University, Princeton, NJ 08543
[2]Columbia University, New York, NY 10027

E-mail: lpku@pppl.gov

Abstract
Characteristics of modular coils for quasi-axisymmetric stellarators that are related to the plasma aspect ratio, number of field periods and rotational transform have been examined systematically. It is observed that, for a given plasma aspect ratio, the coil complexity tends to increase with the increased number of field periods. For a given number of field periods, the toroidal excursion of coil winding is reduced as the plasma aspect ratio is increased. It is also clear that the larger the coil-plasma separation is, the more complex the coils become. It is further demonstrated that it is possible to use other types of coils to complement modular coils to improve both the physics and the modular coil characteristics.

PACS: 52.55Hc, 52.55.-s, 28.52.-s

1. Introduction

Coil systems for stellarators must provide both poloidal and toroidal fields to produce rotational transform and to shape plasmas; consequently they are inherently more complex than the planar coils in tokamaks. For quasi-symmetric stellarators, magnetic field strengths follow certain two-dimensional symmetry, B(s, θ, ϕ) = B(s, $\theta-\gamma\phi$), but the geometric shape of the plasma may be entirely three-dimensional. Here, s is a radial coordinate labeling the flux surface, θ and ϕ are poloidal and toroidal angles, respectively, and γ is a constant. In such quasi-symmetric stellarators, particle drift orbits align (almost) with flux surfaces, if they exist, so that particle trajectories are well confined [1]. Quasi-symmetric stellarators are able to provide toroidally confined plasmas stable to the magnetohydrodynamic (MHD) disturbances and free of disruptions. They have been considered as potential candidates for fusion power plants [2]. In general, coils for such stellarators do not possess symmetry properties other than the stellarator symmetry, X(θ,ϕ)=X($-\theta$,$-\phi$).

A variety of coil topologies are generally available in quasi-symmetric stellarators for a given plasma configuration. In particular, modular coils which combine toroidal and poloidal field coils into one system are considered to be the most practical solution to the coil problem in quasi-symmetric stellarators. They have been chosen in the design for quasi-axisymmetric stellarators NCSX [3] and ARIES-CS [4], quasi-helically symmetric stellarator HSX [5], quasi-poloidally symmetric stellarator QPS [6], and quasi-omnigeneous stellarators W7X [7] and HSR [8]. The geometry for these coils is a complicated function of the shape of the plasma and the location of the coils. Simplified design guidelines or analytic approaches using algebraic or trigonometric functions have not been found.

In tokamaks the planar toroidal and poloidal field coils may generally be placed at arbitrary distances away from the plasma. In stellarators the placement of coils must be carefully chosen since the complexity of the coil winding increases with the increased distance from the plasma. In stellarators the boundary shape of the plasma determines most of the physics properties. Typically 20-30 geometric variables may be used to define the boundary shape once the plasma aspect ratio, rotational transform and number of field periods are chosen. Different combinations of variables will modify not only the properties of the plasma but also the topology of the coils. It is not at all clear how one would take coil considerations in the process of designing a plasma configuration.

In our exploration of plasma configurations for quasi-symmetric stellarators, we often observed that, for a particular equilibrium of interest, there exist many neighboring equilibria that possess similar physics properties and have similar geometric shapes. Taking advantage of this observation, in reference [9], we have made a systematic study for quasi-axisymmetric (QAS) configurations -- configurations whose magnetic field strengths are essentially invariant in the toroidal direction on a given flux surface -- in three field periods with different levels of rotational transform and plasma aspect ratios. We showed that modular coils for configurations with larger aspect ratios tend to have lesser toroidal excursion and that it is possible to use a single set of trim coils along with planar toroidal field coils to produce MHD stable plasmas of different levels of rotational transform by varying currents in these trim coils. This report summarizes our recent efforts to extend that study to a larger set of parameters, including the number of field periods, plasma aspect ratio, rotational transform and distance separating the coil winding surface from the plasma boundary surface, again for QAS, emphasizing the qualitative relationships between these parameters and the characteristics of the modular coils. By establishing the relationships we hope to better deal with the complexity issue in the coil design for quasi-symmetric stellarators.

In section 2 we discuss plasma configurations of different aspect ratios in 2, 3 and 4 field periods. These configurations were developed as the basis for comparison of coils. In section 3 we compare characteristics of modular coils for these plasma configurations. We first hold the rotational transform per field period and the aspect ratio per field period fixed to study the effect of the number of field periods. We then compare configurations with a given aspect ratio with fixed rotational transform per field period. And, lastly, we compare coil characteristics for different aspect ratios with a given level of rotational transform and number of field periods.

Although modular coils are the most practical choice for quasi-symmetric stellarators, there may be situations where using other types of coils to complement modular coils is advantageous. In reference [9] we showed that it is possible to design many different plasma configurations by using a fixed set of windowpane coils together with planar toroidal field coils. For a given plasma configuration, it is possible to use windowpane or other types of coils to simplify modular coils as well. In section 4 we illustrate some of the possibilities for using mixed coil types in the design of QAS. Section 5 gives the summary and conclusions.

2. Plasma configurations for 2, 3 and 4 field periods

To enable comparisons of both plasmas and coils on the same basis, we first developed configurations of 2, 3 and 4 field periods with similar characteristics, including the aspect ratio per field period, rotational transform per field period, plasma beta ($\beta=2\mu<p/B^2>$), stability properties to the MHD perturbations and the degree of quasi-symmetry. To the extent possible, we have selected Fourier harmonics describing the boundary shape of the underlying equilibrium as close as we could, subject to the aforementioned constraints. We then extended the landscape

to other plasma aspect ratios. In reference [9] we have discussed the physics significance of deploying different levels of rotational transform in axi-symmetric plasmas using a sequence of three field period configurations as illustrations. Here we select two rotational transform levels for the discussion of coil characteristics. These will be discussed below.

For the base configurations, the plasma aspect ratio, $A_p=R_p/a_p$, was chosen to be two for each field period. Here R_p and a_p are the average plasma major radius and minor radius, respectively. Two levels of rotational transform supplied by the external coils were chosen: ι~0.1 and 0.15 per field period. These configurations were designed to be stable to the external kink modes and the Mercier modes at β=4% as indicated by the analysis using the linear ideal MHD stability code TERPSICHORE [10]. These configurations all have a magnetic well in excess of 2% in the absence of the plasma pressure. Equilibrium solutions were obtained from VMEC [11] with the prescribed boundary Fourier coefficients. For $\iota \sim 0.1$ per field period, the configurations were chosen to have a large elongation with the toroidally averaged value of about 1.9. They are essentially stable to the ballooning modes as well because of the large elongation. The cases for $\iota \sim 0.15$ per field period were designed to have a larger triangularity but smaller elongation. The effective helical ripples used to judge the quality of quasi-axisymmetry, as calculated by the NEO code [12], are all less than ~1% in the bulk of the plasma volume though not necessarily near the edge. Configurations in three-field periods (N_p=3) with A_p/N_p=2 were derived first to serve as the reference. Fourier coefficients that describe the plasma boundary, as well as the plasma current, were then adjusted accordingly to obtain configurations in two and four field periods and at other plasma aspect ratios. Plasma cross sections derived in this way in 2, 3 and 4 field periods with A_p=2 per field period are shown in figures 1 and 2 for ι~0.1 and 0.15, respectively. The rotational transform we refer to hereafter will be understood as that due to the plasma shaping given in one field period.

We describe plasma boundaries using the Garabedian representation [13]:

$$R + iZ = e^{2\pi i u} \sum \Delta_{m,n} e^{-2\pi i (mu - nv)} \qquad (1)$$

Here, R and Z are the radial and axial components of cylindrical coordinates, m and n are the poloidal and toroidal mode numbers, and u and v are the normalized poloidal and toroidal angle-like variables, $0 \le u < 1$ and $0 \le v < 1$ ($2\pi u = \theta$, $2\pi v/N_p = \phi$, θ and ϕ being the poloidal and toroidal angles, respectively). In this notation, the coefficient $\Delta_{0,0}$ is a measure of the plasma minor radius and $\Delta_{1,0}$ the major radius. The helical excursion, elongation and triangularity in the plasma shaping may be described by the m=1, 2 and 3 terms, respectively. The major Fourier terms with $\Delta_{m,n}/\Delta_{0,0} > 1\%$ are given in tables 1 and 2 for the configurations shown in figures 1 and 2. The terms with large magnitudes, which control mostly the elongation and triangularity, are similar by design in each of the tables, e.g. $\Delta_{2,0}$, $\Delta_{2,1}$, $\Delta_{3,0}$, although the terms $\Delta_{-1,0}$, and $\Delta_{-1,-1}$ that modify the indentation have somewhat larger differences. In particular, in the two field-period configurations the stability constraint for the kink modes requires more plasma shaping because the overall smaller rotational transform leads to larger amounts of bootstrap current that drive the instability. In these two field-period configurations the increased shaping also comes from other triangular and square terms in addition to $\Delta_{-1,-1}$, leading to a more rectangular-like cross section at the beginning of a field period for the ι~0,1 case and a more pointed cross section at the half-period for the ι~0.15 case.

Having obtained the base set of configurations, we then further expand the space by increasing and decreasing aspect ratios for both levels of rotational transform. For two field

periods it covers from 3 to 6, for three field periods from 4 to 8, and for four periods from 6 to 12. In figures 3 and 4 are configurations of three field periods with aspect ratios 4, 6 and 8 for $\iota \sim 0.1$ and $\iota \sim 0.15$, respectively.

We must emphasize that these are not the only possible configurations, nor are they all that satisfactory in every respect. Our use of the three-field period configuration as the reference point for developing configurations of other field periods and aspect ratios constrains the landscape that can be searched. The configurations discussed in this report were designed to be only sufficient for the purpose of understanding the relations between coil and plasma characteristics.

3. Characteristics of modular coils for the 2-, 3- and 4- field period plasma configurations

To compare characteristics of coils, it is reasonable to require that all configurations have the same fusion power, temperature and density profiles, magnetic field strength, plasma beta and distance separating the plasma from the winding surface of the coils, including the space needed for tritium breeding blanket and coil protection shielding. The coils are assumed to be wound on a continuous toroidal surface which is conformal in shape to the plasma boundary but displaced uniformly from the plasma by a fixed distance.

Coils necessary to support a plasma configuration of known boundary shape may be derived by minimizing the normal component of the magnetic fields on the plasma surface from currents both in the plasma and on the winding surface. The current densities on the winding surface, $\boldsymbol{J}$, may be represented by a scalar current potential, κ,

$$\boldsymbol{J} = \hat{\boldsymbol{n}} \times \nabla \kappa \qquad (2)$$

Here, $\hat{\boldsymbol{n}}$ is a unit vector normal to the coil winding surface. The procedure of minimizing the normal magnetic fields on the plasma surface for solving the current potential κ has been implemented in the code NESCOIL [14] which is frequently used in the design of stellarator coils. All the coils in the following discussions have been derived from the solutions of this code. The current potential is written as a double Fourier series in poloidal and toroidal angles. The number of Fourier modes for the current potential has been chosen such that both the residue average errors and maximum errors are similar for all the cases studied when the normal magnetic fields on the plasma surface are minimized. Typically, the maximum error was made to be less than 5% of the local field strength and the average error less than 1%. These errors may be further reduced by using more modes in the current potential but the general picture useful for our discussion does not change. Modular coils were derived by dividing the current potential equally with three distinct contours for each field period.

The complexity of coils depends on the harmonic content of the current potential on the winding surface from which the coils are derived [15]. For a given harmonic the magnetic field decays approximately as $(1+\Delta/a_p)^{\gamma}$ with Δ being the separation between coils and plasma and γ a function of the order of the magnetic field harmonic. If stronger high order fields are needed when minimizing the normal magnetic field on the plasma surface, the structure of current potential is expected to become more complex. For a fixed fusion power, which means a fixed plasma volume with our assumed conditions, Δ/a_p is proportional $\Delta \cdot A_p^{1/3}$, or equivalently, for a given aspect ratio per field period, $\Delta/a_p \sim \Delta \cdot N_p^{1/3}$. So, everything being equal, the coil characteristic is expected to be more complex for a larger number of field periods at fixed plasma volume. The precise definition of coil complexity depends on many factors, however. The radius

of curvature in the coil winding may be too small for a small device, but it may no longer be an issue in a large system such as in a power producing reactor. In general, the ease of assembly and disassembly of machine components and the ease of access to the interior of the coil boundary are the desirable features. Coils with lesser toroidal excursion in the winding, larger radius of curvature and smaller current density at a given field strength should be helpful. Instead of focusing on specific coil design requirements, we shall examine coil characteristics only qualitatively and draw general conclusions.

3.1. Coil configurations for same aspect ratio and rotational transform per field period

In figure 5 we compare coils for plasmas with ι~0.1 and Δ=1.4 m when the plasma volume V_p is normalized to 1000 m^3. In figure 6 we compare coils for the same case but with Δ=2.1 m. These two separations cover the range of radial build considered in most fusion power plant designs. In figure 7 the coil geometries are shown for ι~0.15 with Δ=1.4 m (V_p=1000 m^3). In these figures and figures in the following sections, both coil contours on the winding surface in a coordinate system defined by the normalized toroidal and poloidal angles and the top view of the coils in Cartesian coordinates are displayed.

The contours in figures 5 to 7 indicate that, for fixed A_p/N_p and Δ, the coil characteristics look similar. For configurations having larger numbers of field periods the poloidal spectrum in the current potential is generally richer due to the $N_p^{1/3}$ dependence discussed above, but in coil winding the minimum radius of curvature tends to be larger because of the larger major radius at fixed plasma volume. A smaller fusion power plant requires a smaller coil aspect ratio, $A_c \equiv R_p/\Delta$. If A_p/N_p is fixed, A_c scales as $N_p^{2/3}$ so that smaller plants favor smaller numbers of field periods. The total rotational transform is proportional to the number of field periods for a given rotational transform per field period so that larger numbers of field periods may be more favorable from the standpoint of particle confinement. As mentioned before, coils with larger Δ will be more complex because higher order harmonics in the current potential have stronger presence due to the faster decay of the high order fields they produce, but a larger Δ leads to a smaller A_c so that fusion power plants may be made more compact, hence cheaper in terms of the cost of electricity. The best configuration will ultimately be determined by the systems analysis when all the requirements are defined.

3.2. Coil configurations for same rotational transform per field period and same overall aspect ratio

Given the same fusion power, the same temperature and density profiles, the same magnetic field and plasma beta, the size of a device is determined by the overall aspect ratio, irrespective of the number of field periods that a particular device may have. In figure 8 we compare coil characteristics for configurations with an overall aspect ratio 4 that have the same rotational transform ι~0.1 and the same blanket and shield thickness, Δ~1.4 m (V_p=1000 m^3), in 2 and 3 field periods. In figure 9 we compare coil characteristics for the same configurations but with a larger coil to plasma separation, Δ~2.1 m (V_p=1000 m^3). In figure 10 coil characteristics are compared for the 3 and 4 field period configurations with an overall plasma aspect ratio 8 and with ι~0.1 and Δ~2.1 m (V_p=1000 m^3). In figure 11, coil characteristics are compared for configurations with a plasma aspect ratio 6 and with ι~0.15 and Δ~1.4 m (V_p=1000 m^3) in 3 and 4 field periods.

In general, configurations having the same plasma aspect ratio but more field periods tend to render coils with more pronounced toroidal excursion. The surface current densities tend to be higher and the minimum radius of curvature smaller. For a given plasma aspect ratio, the aspect ratio per field period becomes smaller with more field periods, resulting in the increased

toroidal mode coupling. Magnetic fields due to coils at a given toroidal location on the plasma surface have similarly stronger coupling from neighboring coils. Therefore, for configurations of the same major radius and coil-to-plasma separation, the consideration of coil complexity favors a smaller number of field periods. For the rotational transform, however, it may be more advantageous to have more field periods since the coil complexity tends to increase as the rotational transform per field period is increased.

3.3. Coil configurations for same rotational transform per field period and same number of field periods

For the same overall rotational transform, fusion power, blanket and shielding thickness, configurations with smaller plasma aspect ratios will be smaller with the size scaling $V_p \sim A_p^2$. Correspondingly, the cost of electricity of such fusion power plants will be smaller. We illustrate in figures 12 and 13, for the two plasma-coil separations, coil characteristics for the 4 field-period configurations with $\iota \sim 0.1$ in three different plasma aspect ratios, 6, 8 and 12. In figure 14, coil characteristics are compared for the three field-period configurations with $\iota \sim 0.1$ and $\Delta \sim 2.1$ m for $V_p = 1000$ m^3 in aspect ratios 4, 6 and 8. In figure 15, coil characteristics are displayed again for the three field-period configurations but with $\iota \sim 0.15$ and $\Delta \sim 1.4$ m ($V_p = 1000$ m^3). Finally, we show coil characteristics for the two field period configurations, also with $\iota \sim 0.15$ and $\Delta \sim 1.4$ m, in aspect ratios 3, 4 and 6. It is clearly seen from these configurations, which cover a wide range of aspect ratios, rotational transform and numbers of field periods, that the larger the separation between the plasma and coil is, the more complex the coils become, but for a given plasma to coil separation, the larger the aspect ratio is, the lesser excursion toroidally the coils will have. The content of poloidal harmonics in the current potential among configurations of different aspect ratios appears to be similar. The smaller toroidal excursion in coils for larger aspect ratio configurations is due to the relatively smaller poloidal fields in larger aspect ratio configurations at a given plasma beta. The smaller toroidal excursion in the coil winding makes the tasks for machine assembly and maintenance less complex.

4. Use of mixed types of coils

Modular coils have been chosen in the design of modern transport-optimized stellarators for practical reasons, but in many circumstances the use of only modular coils makes it difficult to meet some physics or engineering objectives. In such situations, use of other types of coils as a complimentary system may be more practical and economical. One example is that, in NCSX, the radial profile of the bootstrap current at high beta may produce shear reversal near the edge of the plasma because the pressure gradient is reduced there and the shear from plasma shaping is not strong enough to compensate for the reduced current density. The shear reversal is not desirable if there are resonances nearby, making the plasma prone to breakup into stochastic and island regions. A high order perturbed field may be introduced to remove the shear reversal, but other properties, such as quasi-axisymmetry, are compromised when the shear, $1/\iota \cdot d\iota/ds$, outside the reversal region becomes less than -0.15. Even if high order fields can be introduced, designing coils using a single modular system may require high order harmonics and good precision.

In figure 17, we show the last closed magnetic surface for both the reference equilibrium of NCSX and a perturbed equilibrium whose total magnetic shear is monotonically increasing. The rotational transform is given in figure 18 in which the transform due to the plasma shaping as well as the total transform including the internal contribution from bootstrap currents at 4% beta are shown using the reference pressure profile of the NCSX design [3]. It is seen that a small perturbation is able to remove the shear reversal in this case. If one attempts to construct modular coils for the perturbed configuration, however, one finds that the coils become much more

complex. This is shown, as an example, in figure 19 where the winding surfaces are given and in figure 20 where contours of coil winding for both unperturbed and perturbed cases are shown. In this example the winding surface is conformal to the boundary of the reference plasma but is uniformly displaced by a distance $\Delta \sim 0.16R_p$ (or ~1.5 m for V_p=1000 m^3). The current potentials were solved using the NESCOIL code with six toroidal and six poloidal modes. The resulting residue errors in the normal magnetic fields on the plasma boundary surface are ~0.7% on average and ~5% at the maximum location. The coil windings show high order twists and turns and clearly much more so in the perturbed configuration.

Instead, we now introduce a set of dipole coils arranged as sixteen by sixteen arrays of square loops in a plane defined by the normalized toroidal and poloidal angles on a conformal surface at a distance half way between the last closed magnetic surface of the plasma and the winding surface for the modular coils. The currents in these dipoles can be optimized such that not only the shear reversal is removed but the modular coils can also be made simpler. This is shown in figure 21, where we show the contours of the modular coils constructed using three toroidal modes and three poloidal modes. The current densities in the dipole loops are also shown in figure 21. The peak current density occurs toroidally at an angle which is about 120 degrees (of one field period) from the crescent shaped cross section and poloidally near the top (largest height) of the cross section at this 120 degree toroidal angle. The current in the loops at the location of the peaked density is about 10% of the poloidal current carried by the modular coils. A comparison is given in figure 22 for the rotational transform based on the equilibrium using these coils and that from the perturbed plasma boundary shown in figure 18. The two methods yield nearly identical profiles for the rotational transform, both monotonically increasing. The modular coils with the dipole loops are much less complex compared to those in figure 19. We note, however, that the current densities in the dipole coils display a steep gradient with localized peaking in a narrow band. Further optimization to regularize the current distribution may be necessary to reduce the potentially large local magnetic forces.

To further illustrate the potential use of mixed coil types to reduce the complexity of modular coils, we now use the three-field period, aspect ratio 4 configuration discussed in section 2 as an example. The modular coils designed on a winding surface whose separation from the last closed magnetic surface of the plasma is ~ 1.5 m at the inboard mid-plane and ~3.0 m at the outboard mid-plane when V_p=1000 m^3 will not be convenient for assembly in either full or half field periods because of the large toroidal excursion of the winding, as shown in figures 23 and 24. The toroidal excursion of the winding may be reduced in several different ways: (1) using the strategically placed trim coils to complement the modular coils, shown in figure 25, where the trim coils are mounted on a surface outside the modular coils with a distance from the plasma further displaced by ~0.5 m (V_p=1000 m^3); (2) strategically straightening the modular coil winding but supplemented them with trim coils, shown in figure 26, where the trim coils are placed closer to the plasma at a distance about 0.5 m from the last closed plasma surface (V_p=1000 m^3) to reduce coil currents; (3) using wavy poloidal field coils together with modular coils, shown in figure 27, where the poloidal coils are on a surface ~0.5 m outside the modular coils (V_p=1000 m^3); and (4) using saddle coils along with modular coils, shown in figure 28, again on a surface about ~0.5 m outside the winding surface for the modular coils (V_p=1000 m^3). In any one of these cases, the interference due to the toroidal extension of the coil winding is removed to enable either a full- or half-period assembly. We note, however, that the purpose here is to show that topologically it is possible to simplify modular coils when combined with other type of coils. The additional coils inevitably will introduce other issues, such as those associated with coil leads and supports. The currents in the supplemental coils are of the same order of magnitude as those in the modular coils except when these coils are placed closer to the plasma as in case (2) where the currents in the trim coils are about one tenth of those in the modular coils.

Ultimately, the best solution to mitigate the overall coil complexity will rest on the design optimization with all aspects of manufacturing and installation taken into consideration.

5. Summary and Conclusions

A systematic study has been made to examine variations in the characteristics of modular coils that are related to the rotational transform, plasma aspect ratio, number of field periods and distance separating coils from the plasma, for quasi-axisymmetric stellarators. Plasma configurations having similar MHD stability and symmetry properties in two, three and four field periods were first developed with different levels of rotational transform. Modular coils were then constructed on the winding surfaces which were conformal to the plasma surface but displaced uniformly in all poloidal and toroidal angles by a fixed distance. The current potential on the winding surface was solved such that the normal magnetic fields on the plasma surface were minimized with the number of poloidal and toroidal modes in the current potential chosen to yield similar residual errors for different cases. Coils of equal currents were derived from the current potential with three coils per half-period. Comparisons of coil characteristics were made on the basis of the same plasma volume, plasma beta, magnetic fields and rotational transform per field period. It was observed that, given the same plasma aspect ratio per field period at the same coil-plasma separation, coil characteristics are similar, particularly with respect to the toroidal winding excursion. It was also observed that, given the same plasma aspect ratio, coil complexities tend to increase with the increased numbers of field periods for a fixed coil-plasma separation. For a given number of field periods, the toroidal excursion of coil winding is reduced as the plasma aspect ratio is increased. It is also clear that the larger the coil-plasma separation is the more complex the coils become.

In addition, the use of mixed types of coils was also examined. Combining modular and windowpane coils not only could reduce the complexity of modular coils but also may be used to improve plasma characteristics at the same time. This was demonstrated in an example for NCSX where the windowpane coils were used to modify the rotational transform to avoid the shear reversal. Strategically placed dipole coils can also be deployed to relieve the interference among modular coils during machine assembly and maintenance due to the protruding toroidal wings in the coil winding. Finally, we showed that the same objective could be attained by a combination of modular and saddle coils as well as modular and wavy poloidal field coils.

Quasi-symmetric stellarators have the potential to be able to maintain steady-state, disruption-free, MHD stable plasmas at high β. The complexity of coils, however, is generally perceived as compromising the potential. The coil complexity issue cannot be addressed easily without taking into account the many design and cost factors. Systems studies will ultimately be required to find the optimal solution once the basic plasma parameters are chosen. Our study reported here illustrates the richness of the configuration space, for both plasmas and coils, so that there will be flexibility and freedom to optimize a design for it to meet both the physics and engineering objectives.

Acknowledgements

This work was supported by U. S. Department of Energy through the grant ER54333 to Columbia University and the contract DE-AC02-09CH11466 to the Princeton Plasma Physics Laboratory.

References

1. Boozer A 1998 *Physics of Plasmas*, **5(5)** 1647
2. Boozer A 2008 *Plasma Physics & Controlled Fusion* **50** 124005
3. Zarnstorff M, Berry L, Brooks A, Fredrickson E, Fu G Y, Hirshman S, Hudson S, Ku L P, Lazarus E, Mikkelsen D, Monticello D, Neilson G, Pomphrey N , Reiman A, Spong D, Strickler D, Boozer A, Cooper W, Goldston R, Hatcher R, Isaev M, Kessel C, Lewandowski J, Lyon J, Merkel P, Mynick H, Nelson B, Nuehrenberg C, Redi M, Reiersen W, Rutherford P, Sanchez R, Schmidt J and. White R 2001 *Plasma Phys. Control. Fusion* **43**, A237
4. Najmabadi F, Raffray A and ARIES-CS Team 2008 *Fusion Science and Technology* **54(3)** 655
5. Canik J, Anderson D, Anderson F, Clark C,. Likin K, Talmadge J and Zhai K 2007 *Phys. Plasmas* **14** 056107
6. Ware A, Hirshman S, Spong D, Berry L, Deisher A, Fu G Y, Lyon J and Sanchez R 2002 *Phys. Rev. Lett.* **89** 125003
7. Beidler C, Grieger G, Herrnegger F, Harmeyer E, Kisslinger J, Lotz W, Maassberg H, Merkel P, Nuhrenberg J, Rau F, Sapper J, Sardei F, Scardovelli R, Schluter A and Wobig H 1990 *Fusion Technology* **17** 148
8. Beidler C, Harmeyer E, Herrnegger F, Igitkhanov Y, Kendl A, Kisslinger J, Kolesnichenko Y, Lutsenko V, Nuhrenberg C, Sidorenko I, Strumberger E, Wobig H and Yakovenko Y 2001 *Nuclear Fusion* **41** 12 1759
9. Ku L P and Boozer A 2009 *Physics of Plasmas* **16** 082506
10. Anderson D, Cooper W, Gruber R, Merazzi Sand Schwenn U 1990 *Scient. Comput. Supercomput.* **II** 159
11. Hirshman S, Rij W and Merkel P 1986 *Comput. Phys. Commun.* **43** 143
12. Nemov V, S. Kasilov S, Kernbichler W and Heyn M 1999 *Physics of Plasmas* **6** 4622
13. Bauer F, Betancourt O and Garabedian P 1984 "*Magnetohydrodynamic Equilibrium and Stability of Stellarators*" Springer-Verlag, New York
14. Merkel P 1987 *Nuclear Fusion* **27(5)** 867
15. Boozer A 2000 *Physics of Plasmas*, **7(2)** 629

Table 1. Boundary coefficients, $\Delta_{m,n}$, for 2, 3 and 4 field-period configurations with ι =0.1 per field period.

m	n	N_p=2	N_p=3	N_p=4
-1	-1	0.109	0.087	0.065
-1	0	0.100	0.119	0.189
0	0	1.000	1.000	1.000
0	1	0.108	0.099	0.090
1	0	3.445	5.178	7.008
1	1	0.171	0.107	0.122
1	2	-0.020	-0.035	-0.031
2	-1	0.052	0.049	0.055
2	0	-0.321	-0.313	-0.313
2	1	-0.345	-0.350	-0.359
2	2	-0.021	-0.019	-0.010
3	-1	-0.014	-0.020	-0.014
3	0	0.115	0.132	0.135
3	1	0.080	0.069	0.053
3	2	0.062	0.061	0.073
4	0	-0.049	-0.002	-0.025
4	1	-0.050	0.000	-0.009
4	3	-0.028	-0.017	-0.022

Table 2. Boundary coefficients, $\Delta_{m,n}$, for 2, 3 and 4 field-period configurations with ι =0.15 per field period.

m	n	N_p=2	N_p=3	N_p=4
-1	-1	0.240	0.226	0.226
-1	0	0.071	0.132	0.132
0	0	1.000	1.000	1.000
0	1	0.041	0.003	0.003
1	-1	0.076	0.015	0.015
1	0	3.832	5.747	7.663
1	1	0.160	0.023	0.023
2	-1	0.014	0.014	0.014
2	0	-0.213	-0.158	-0.158
2	1	-0.406	-0.385	-0.385
3	0	0.061	0.090	0.090
3	1	-0.025	0.028	0.028
3	2	0.048	0.069	0.069
4	0	-0.001	-0.035	-0.035
4	2	-0.026	-0.014	-0.014
4	3	-0.037	-0.021	-0.021

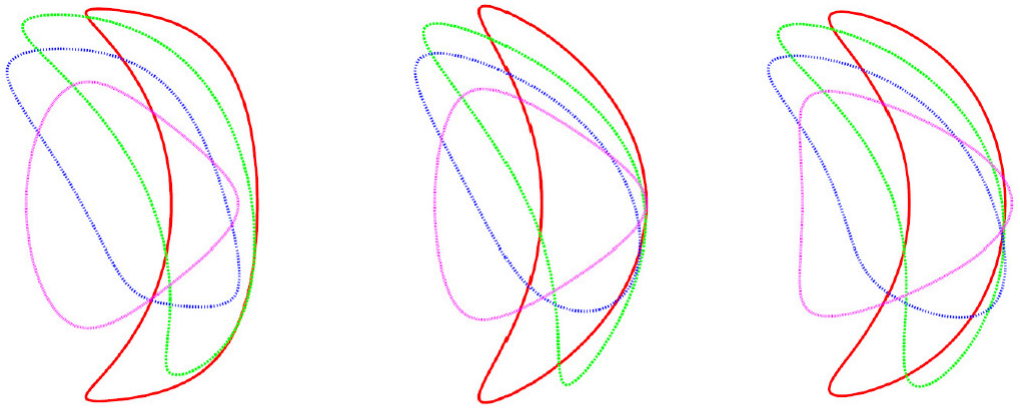

(a) (b) (c)

Figure 1. Cross sections of the last closed magnetic surface in four equal toroidal angles over half-period for the example 2, 3 and 4 field period configurations (frames a, b and c, respectively) with ι~0.1 per field period .

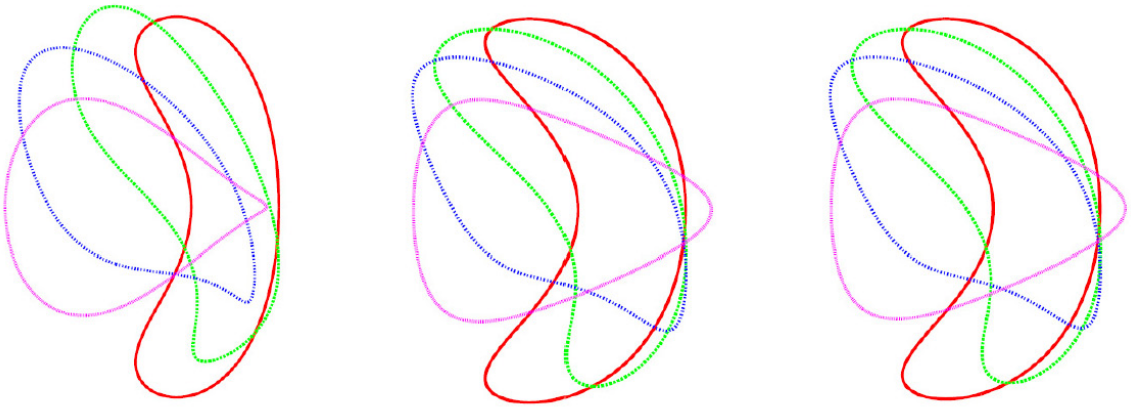

(a) (b) (c)

Figure 2. Cross sections of the last closed magnetic surface in four equal toroidal angles over half-period for the example 2, 3 and 4 field period configurations with ι~0.15 per field period.

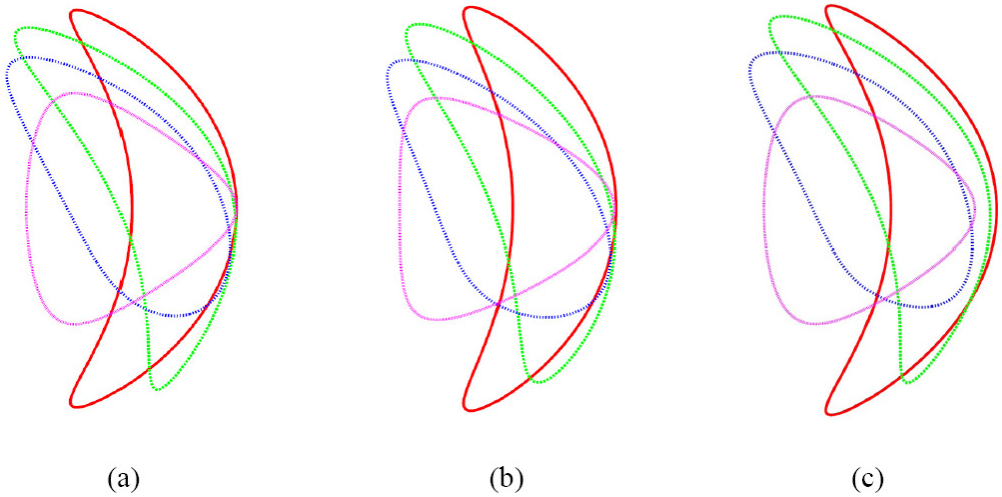

(a) (b) (c)

Figure 3. Cross sections of the last closed magnetic surface in four equal toroidal angles over half-period for the configurtion N_p=3 and ι~0.1 per field period with A_p=4, 6, and 8 (frames a, b and c, respectively).

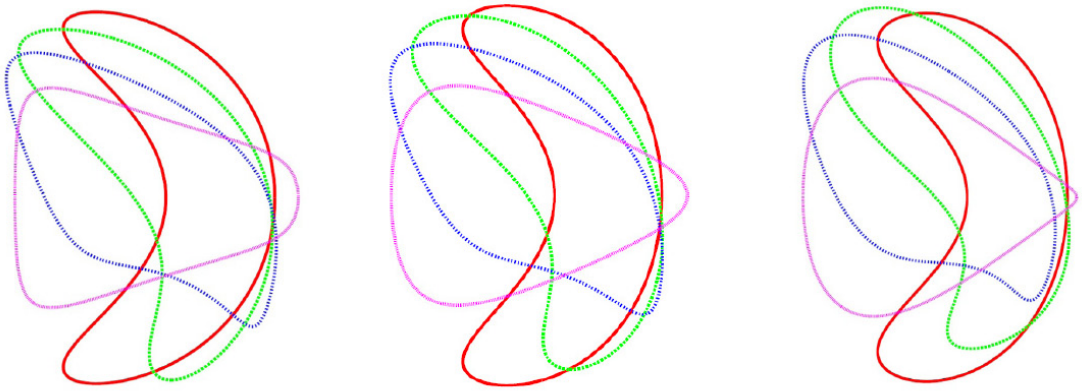

(a) (b) (c)

Figure 4. Cross sections of the last closed magnetic surface in four equal toroidal angles over half-period for the configuration N_p=3 and ι~0.15 per field period for A_p=4, 6, and 8.

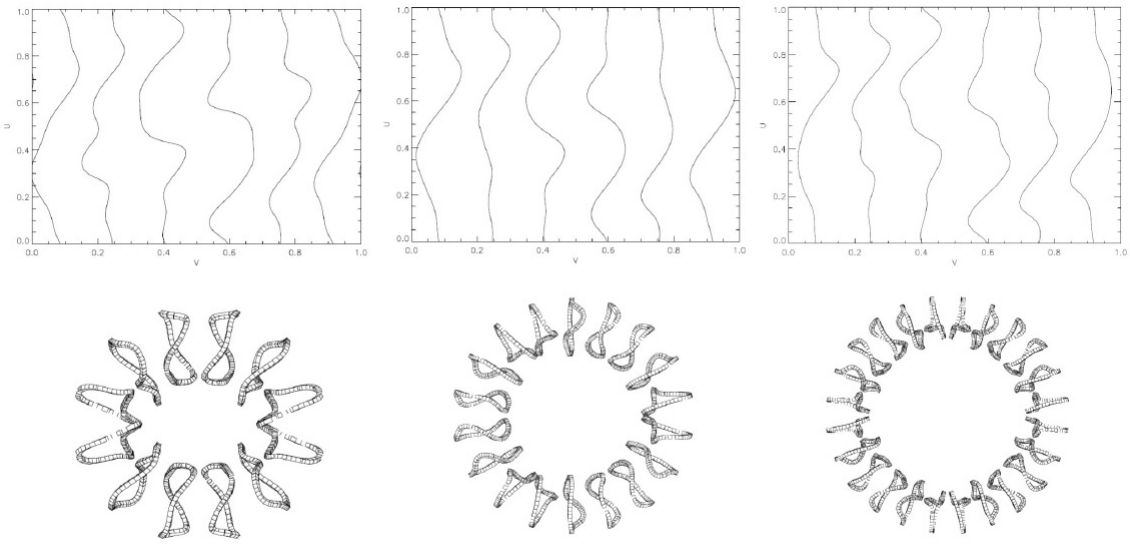

(a) (b) (c)

Figure 5. Comparison of modular coil characteristics for 2-, 3- and 4- field period configurations (frames a, b and c, respectively) with ι=0.1 per field period, A_p=2 per field period and Δ=1.4 m for V_p=1000 m^3. Shown in top row are contours of coils on the winding surface in normalized toroidal and poloidal angles (v and u, respectively) and in bottom row are top views of coils in Cartesian coordinates. For the definition of u and v, see section 2 of text. The major radii of the configurations have been scaled to make all plots about the same size.

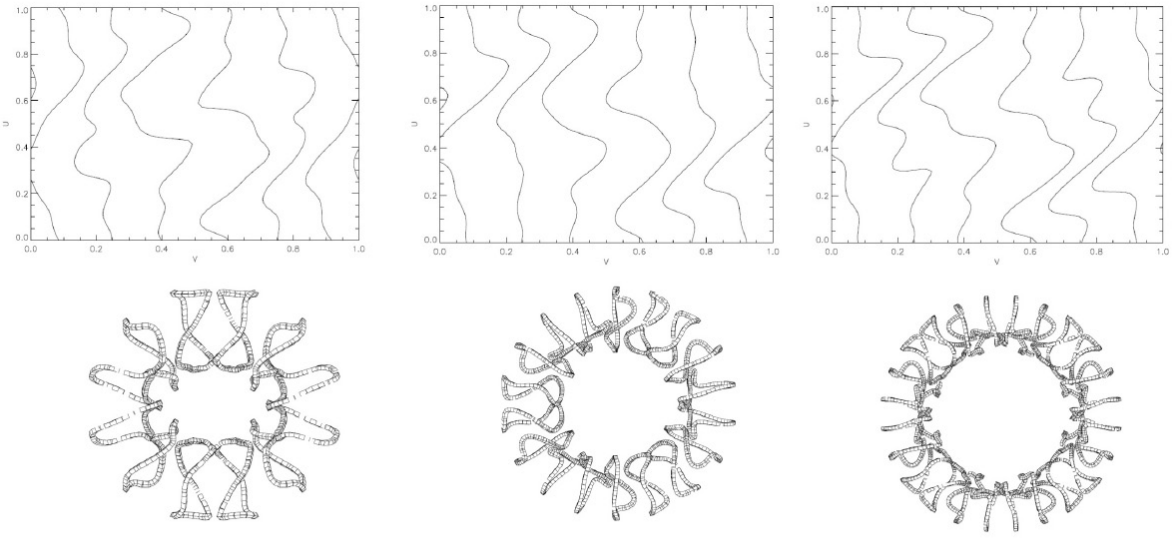

(a) (b) (c)

Figure 6. Comparison of modular coil characteristics for 2-, 3- and 4- field period configurations with ι=0.1 per field period, A_p=2 per field period and Δ=2.1 m for V_p=1000 m^3.

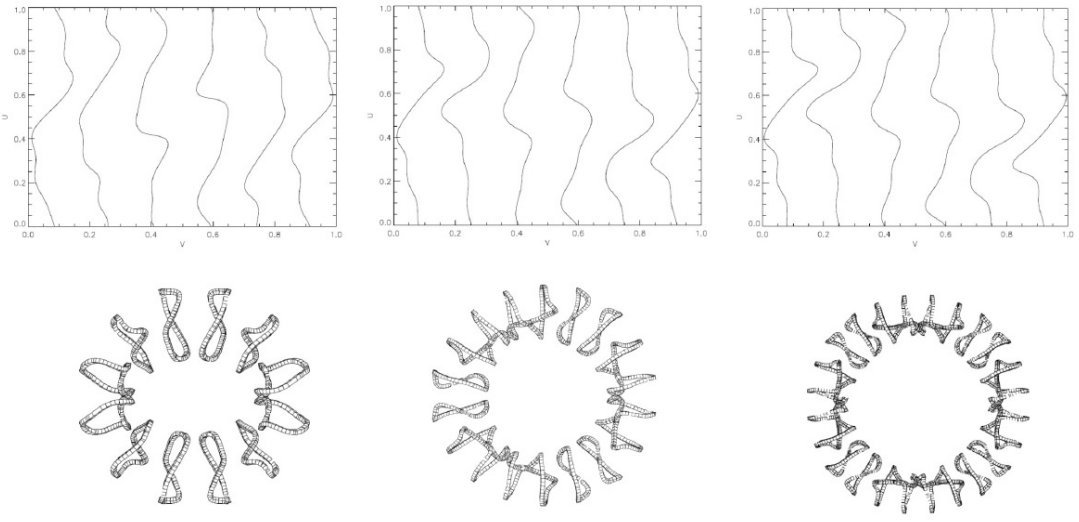

(a) (b) (c)

Figure 7. Comparison of modular coil characteristics for 2-, 3- and 4- field period configurations with ι=0.15 per field period, A_p=2 per field period and Δ=1.4 m for V_p=1000 m^3.

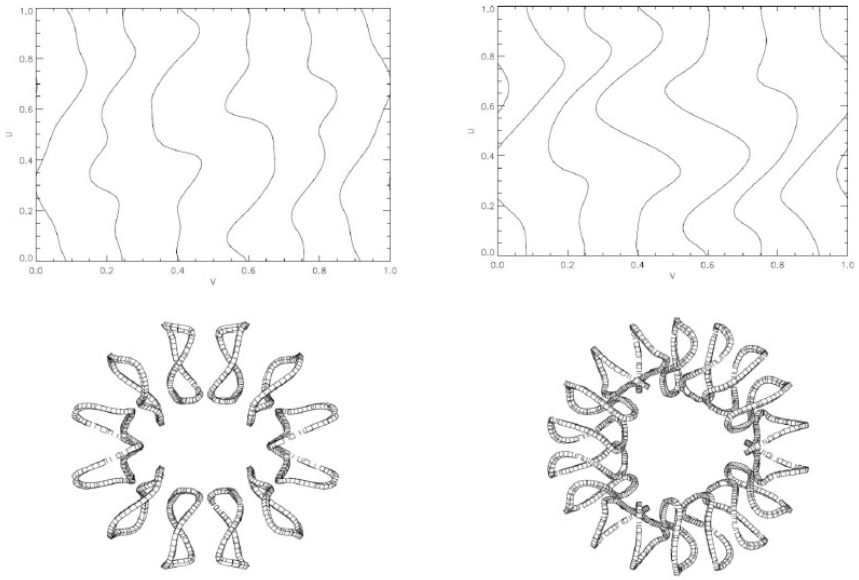

(a) (b)

Figure 8. Comparison of modular coil characteristics for 2- and 3- field period configurations (frames a and b, respectively) with ι=0.1 per field period, A_p=4 and Δ=1.4 m for V_p=1000 m^3.

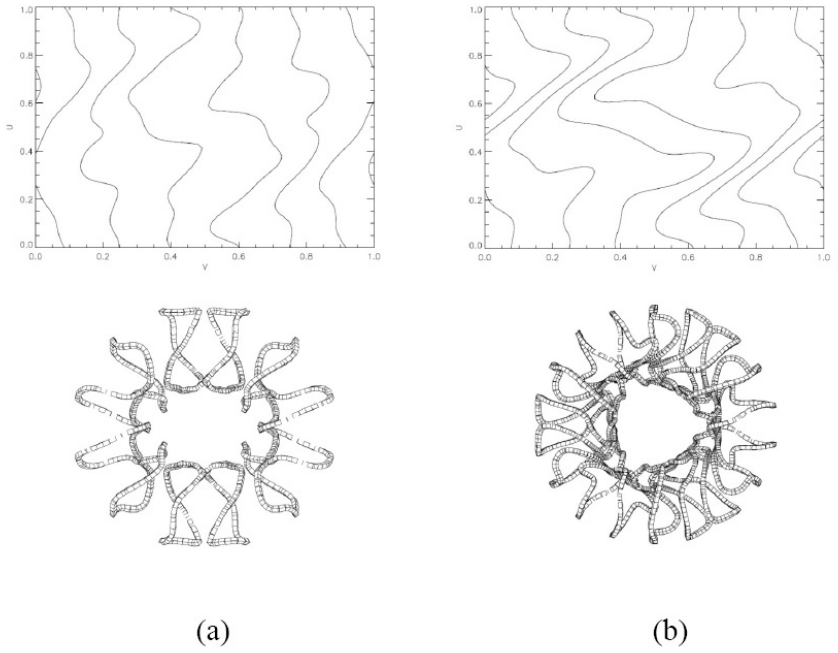

(a) (b)

Figure 9. Comparison of modular coil characteristics for 2- and 3- field period configurations with ι=0.1 per field period, A_p=4 and Δ=2.1 m for V_p=1000 m^3.

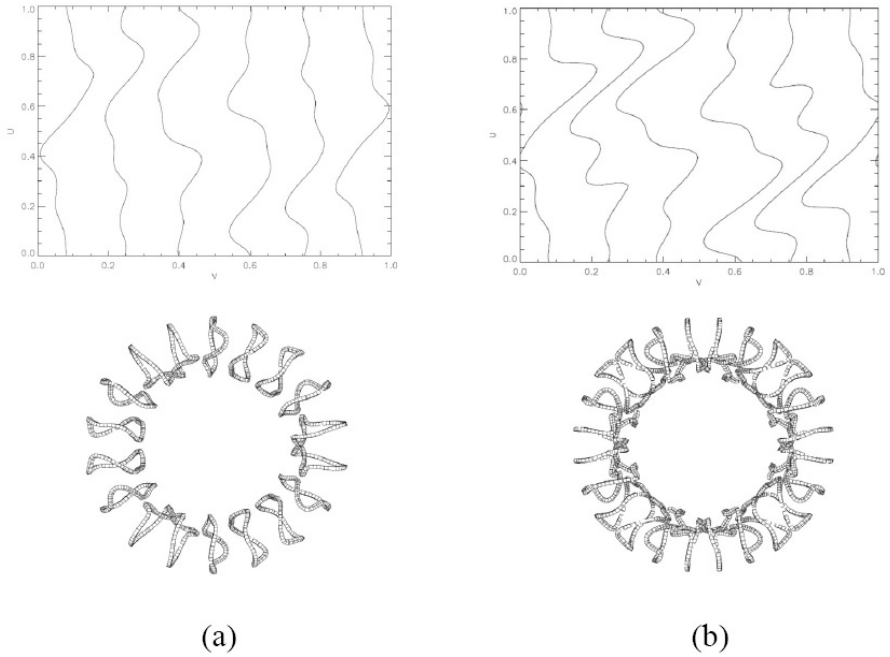

(a) (b)

Figure 10. Comparison of modular coil characteristics for 3- and 4- field period configurations with ι=0.1 per field period, A_p=8 and Δ=2.1 m for V_p=1000 m^3.

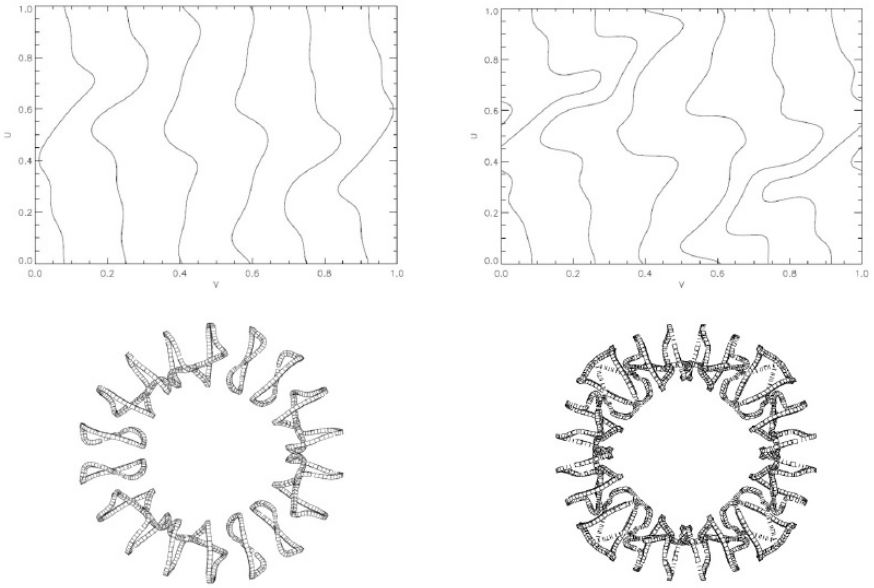

Figure 11. Comparison of modular coil characteristics for 3- and 4- field period configurations with ι=0.15 per field period, A_p=6 and Δ=1.4 m for V_p=1000 m^3.

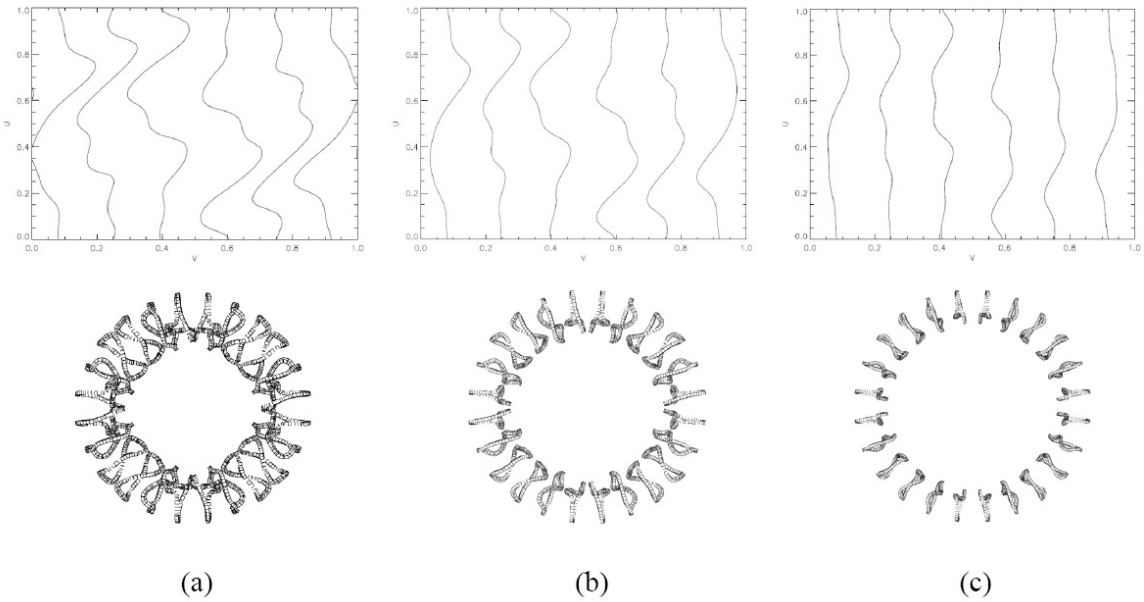

Figure 12. Comparison of modular coil characteristics for 4- field period configurations with A_p=6, 8, 12 (frames a, b and c, respectively) and ι=0.1 per field period and Δ=1.4 m for V_p=1000 m^3.

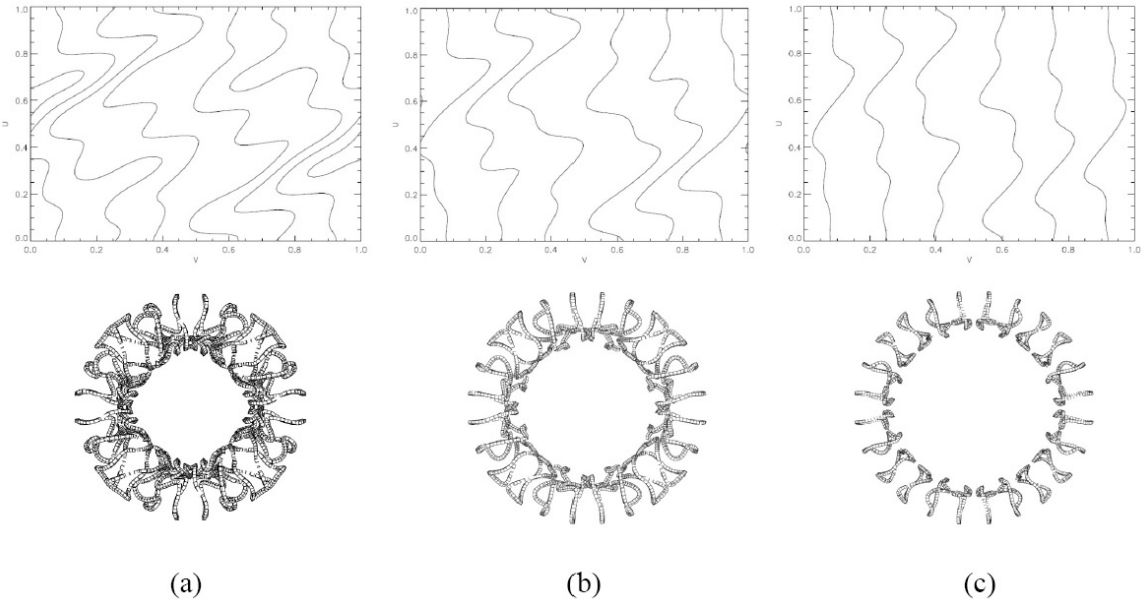

Figure 13. Comparison of modular coil characteristics for 4- field period configurations with A_p=6, 8, 12 and ι=0.1 per field period and Δ=2.1 m for V_p=1000 m^3.

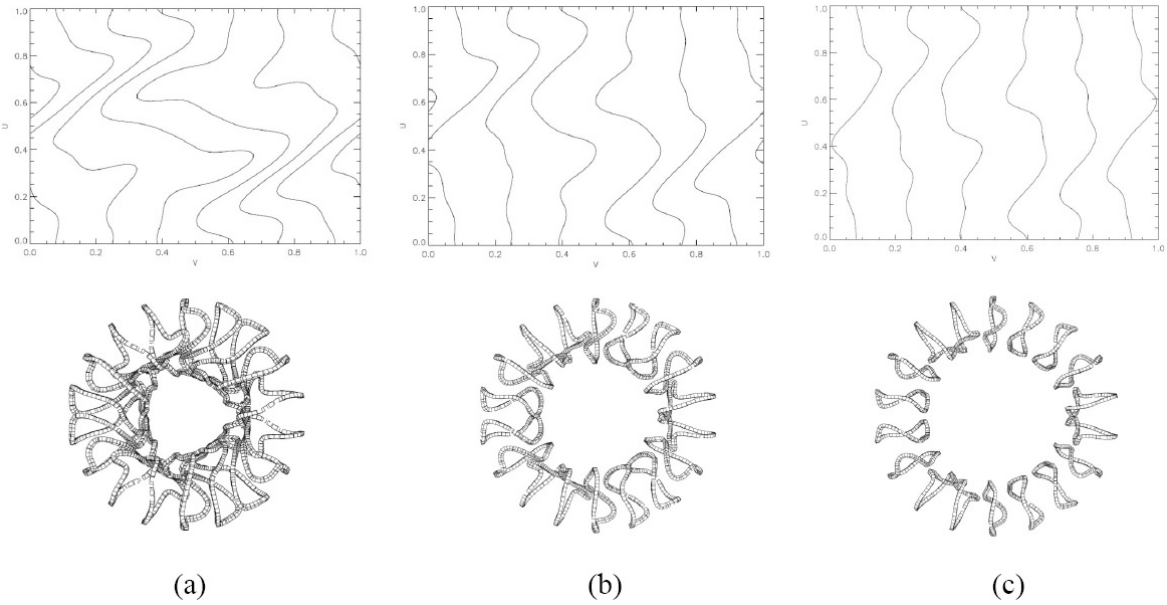

Figure 14. Comparison of modular coil characteristics for 3- field period configurations with A_p=4, 6, 8 and ι=0.1 per field period and Δ =2.1 m for V_p=1000 m^3.

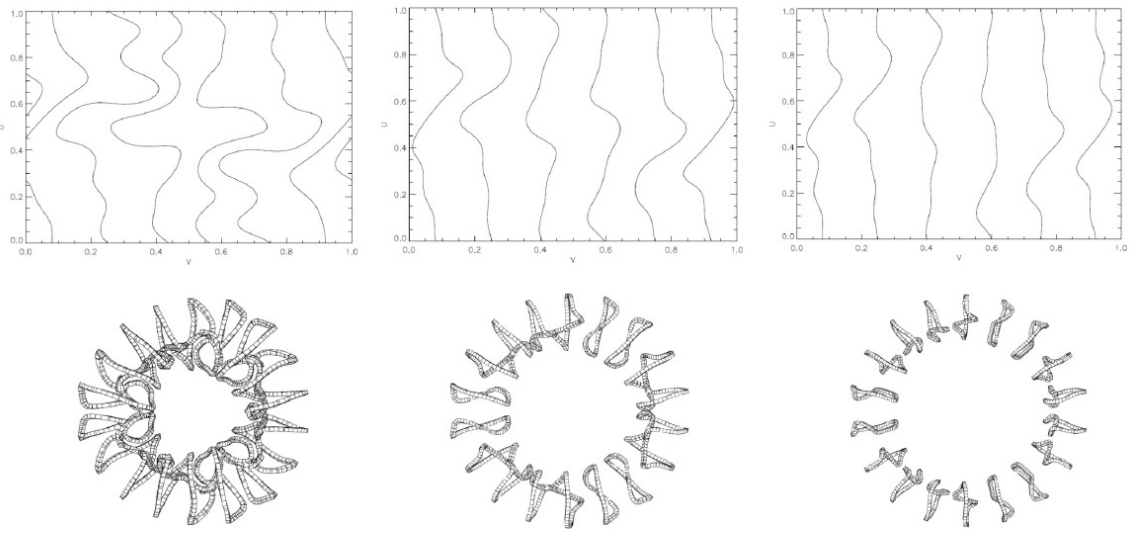

(a) (b) (c)

Figure 15. Comparison of modular coil characteristics for 3- field period configurations with A_p=4, 6, 8 and ι=0.15 per field period and Δ=1.4 m for V_p=1000 m^3.

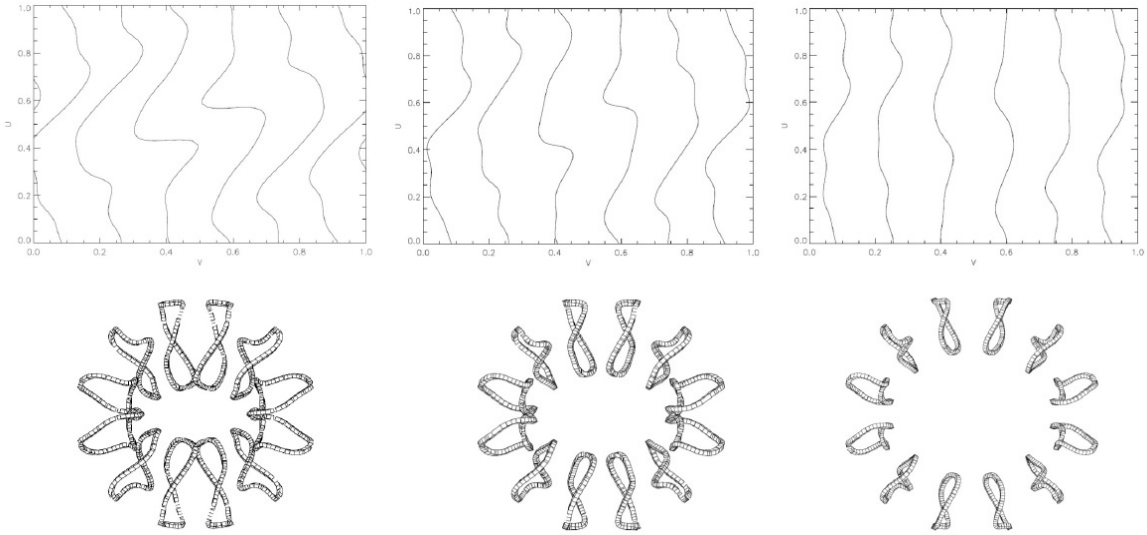

(a) (b) (c)

Figure 16. Comparison of modular coil characteristics for 2- field period configurations with A_p=3, 4, 6 and ι=0.15 per field period and Δ=1.4 m for V_p=1000 m^3.

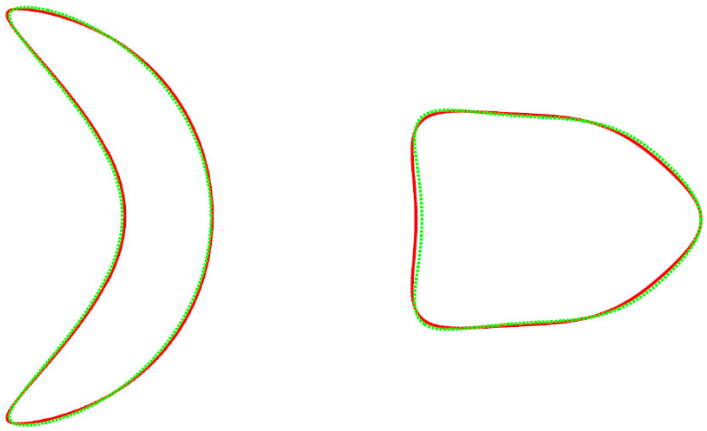

Figure 17. Comparison of the last closed magnetic surface in two toroidal angles for the reference (green) and perturbed (red) NCSX. The perturbation was introduced to make the total rotational transform monotonically increasing at 4% β.

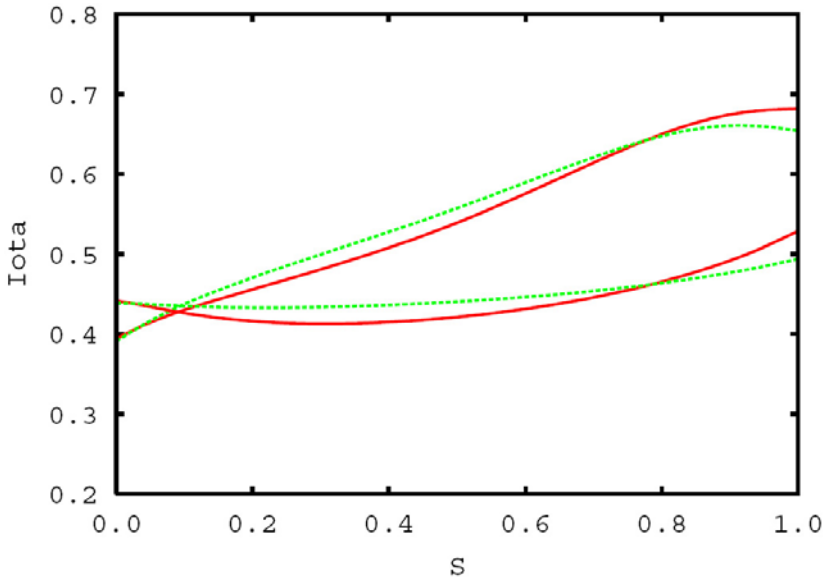

Figure 18. Comparison of the rotational transform for the reference (green) and perturbed (red) NCSX. The top pair of curves is the total rotational transform and the bottom pair is that due to the plasma shaping alone.

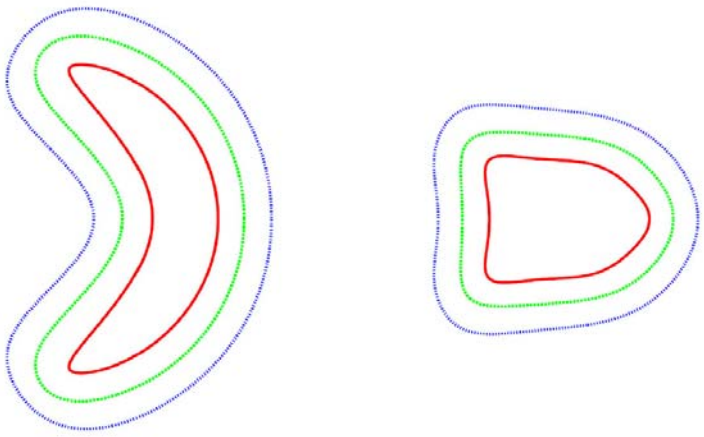

Figure 19. Cross sections of NCSX in two toroidal angles showing the last closed plasma surface (red), the winding surface for window-pane coils (green) and the winding surface for modular coils (blue).

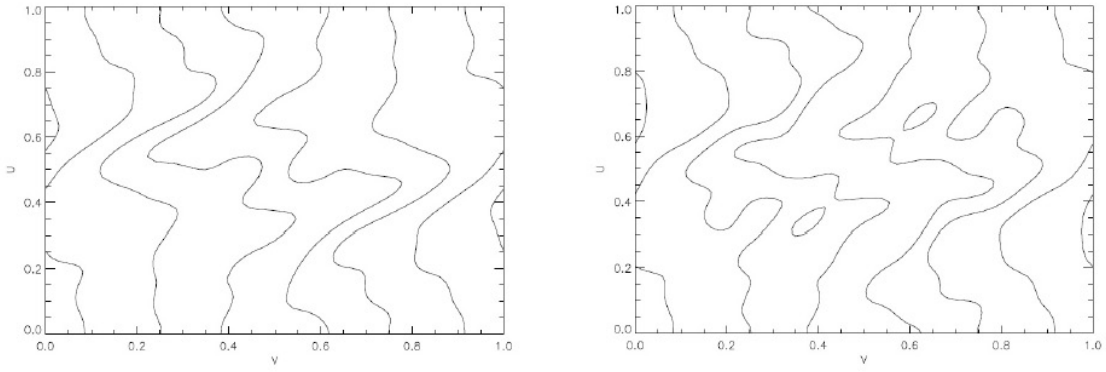

Figure 20. Contours of modular coils for the reference (frame a) and perturbed (frame b) NCSX on the winding surface shown in a coordinate system defined by the normalized toroidal (abscissa) and poloidal (ordinate) angles in one field period.

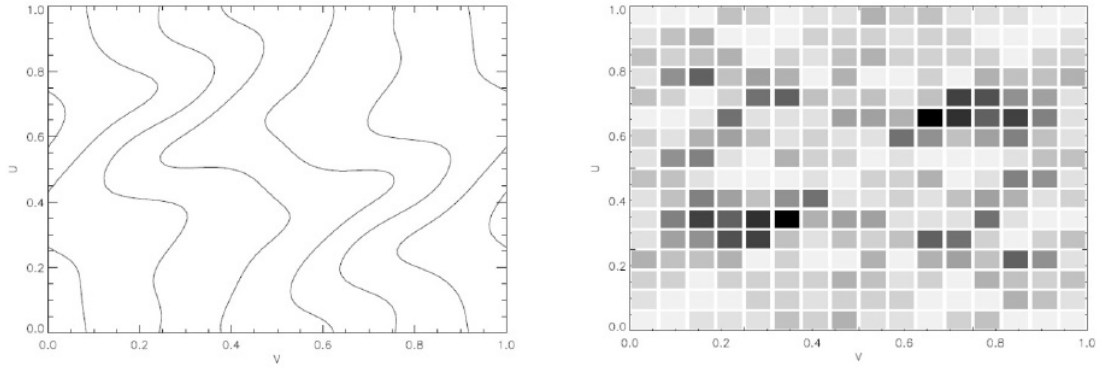

Figure 21. Contours of modular coils (frame a) and current densities in the window pane coils (frame b) for the combined NCSX coil system that removes the shear reversal. The modular coils are designed with the reduced harmonic content. The current density shown for the window pane coils is shaded (black to white) to indicate the relative magnitude. Both frames are shown on the respective winding surfaces in a coordinate system defined by the normalized toroidal (abscissa) and poloidal (ordinate) angles in one field period.

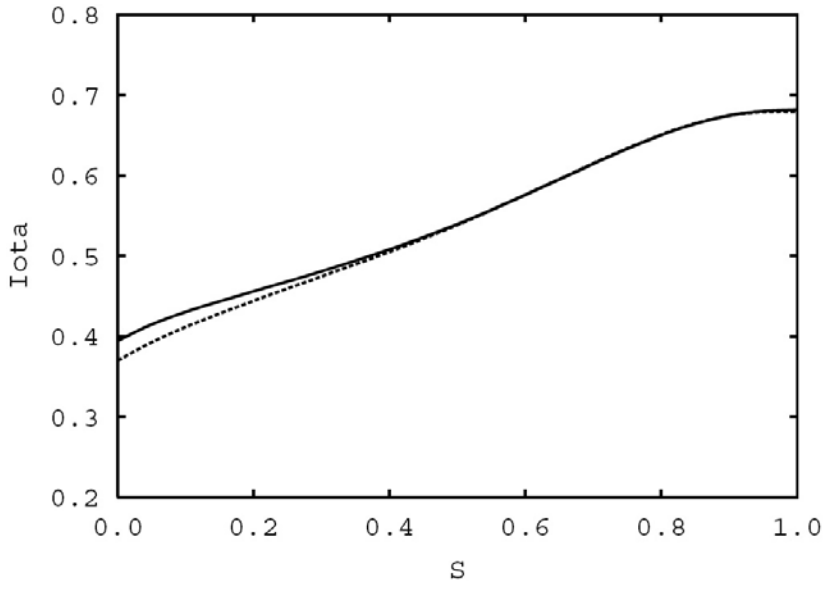

Figure 22. Comparison of the rotational transform for the perturbed NCSX, target (solid) versus using the combined window-pane and modular coils (dotted).

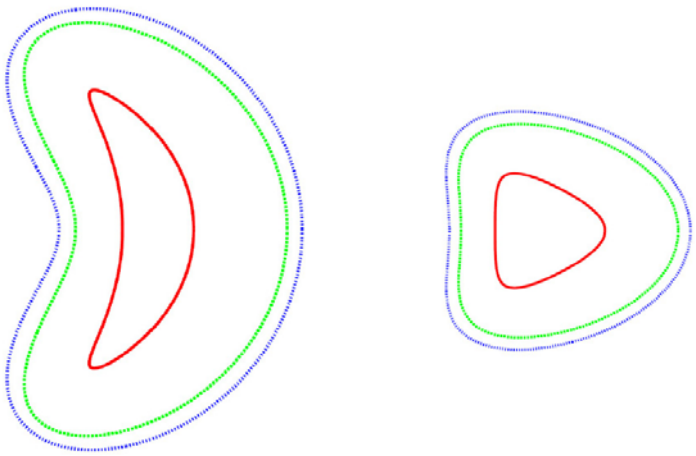

Figure 23. Cross sections of the N_p=3 and A_p=4 plasma (solid-red) discussed in figure 3 and the two winding surfaces for coils. The dashed-green surface is conformal to the plasma surface but is displaced by a distance ~1.5 m at inboard midplane and 3.0 m at outboard midplane from the last closed magnetic surface of the plasma when the plasma volume is scaled to 1000 m^3 with a smooth interpolation at other poloidal angles. The dotted-blue surface is similar to the dashed-green surface except the displacement is further enlarged by 0.5 m (V_p=1000 m^3).

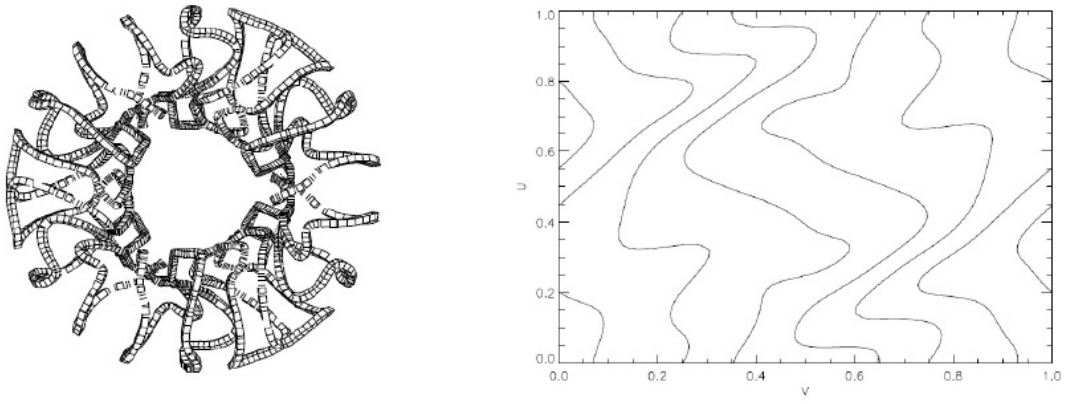

(a) (b)

Figure 24. Modular coils (six coils per field period) designed on the inner winding surface for the configuration shown in figure 23. The left frame (a) is the top view in Cartesian coordinates and the right frame (b) is coils viewed on the winding surface in a coordinate system defined by the normalized toroidal and poloidal angles in one field period. The toroidal excursion of the coils at toroidal angle 0 and 0.5 is such that to assemble or disassemble in full or half period without interference with neighboring coils becomes impossible.

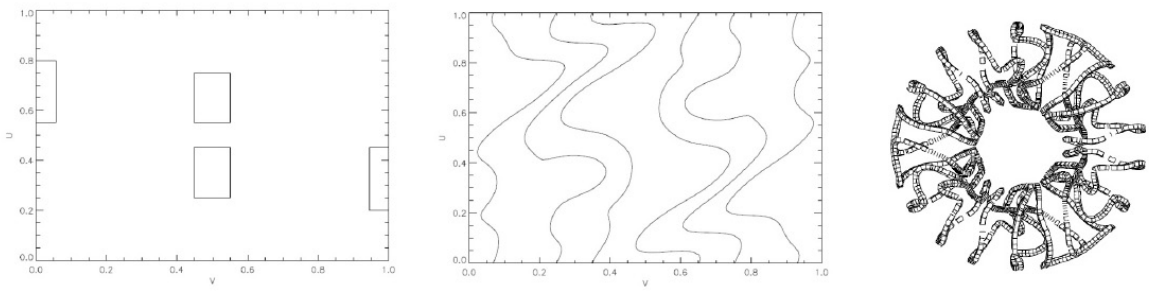

Figure 25. Modification of the coils shown in figure 24 using two pairs of strategically placed trim coils on the outer winding surface (frame a in normalized toroidal and poloidal angles, *v* and *u*) together with the modular coils on the inner winding surface (frames b and c in *u*,*v* and Cartesian coordinates, respectively). For the winding surfaces, see figure 23. Interferences in both inboard and outboard regions at toroidal angle 0 and 0.5 have been removed in the combined system.

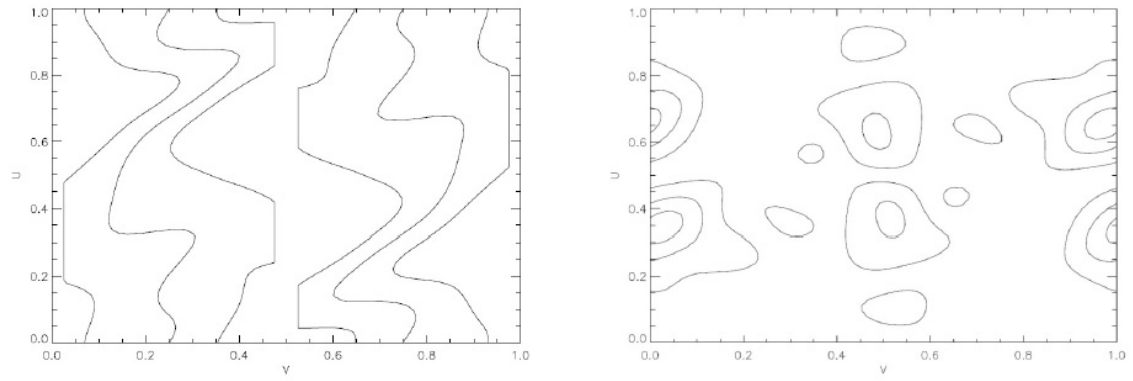

Figure 26. Modification of the coils shown in figure 24 with portion of the modular coils straightened in toroidal angles to prevent interference in assembly/disassembly (frame a) along with the trim coils placed on a conformal surface 0.5 m away from the last closed flux surface of the plasma (frame b) for V_p= 1000 m^3. Both frames are given in normalized toroidal and poloidal angles on the respective winding surfaces.

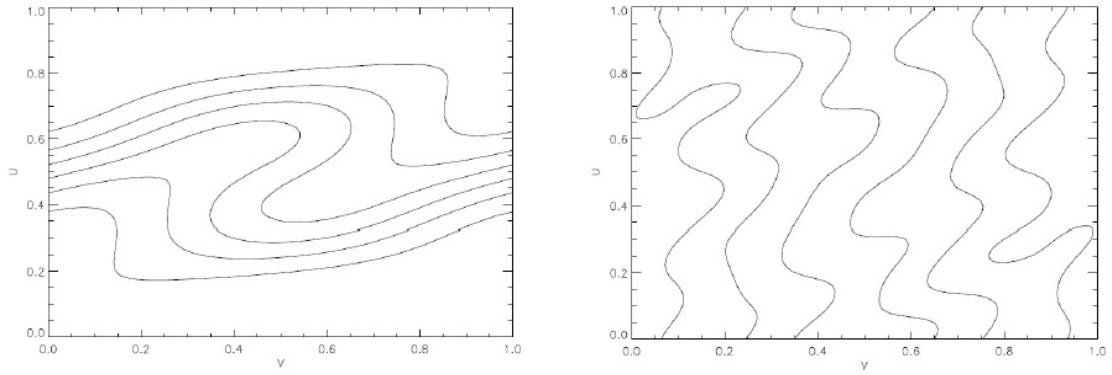

(a) (b)

Figure 27. Modification of the coils shown in figure 24 using wavy poloidal field coils on the outer winding surface (frame a) and modular coils on the inner winding surface (frame b). For winding surfaces, see figure 23.

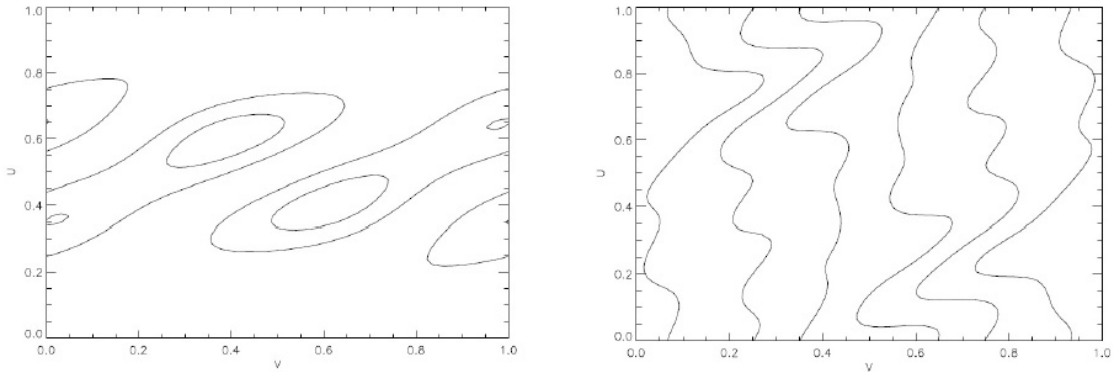

(a) (b)

Figure 28. Modification of the coils shown in figure 24 using saddle coils on the outer winding surface (frame a) and modular coils on the inner winding surface (frame b). For winding surfaces, see figure 23.

The Princeton Plasma Physics Laboratory is operated
by Princeton University under contract
with the U.S. Department of Energy.

Information Services
Princeton Plasma Physics Laboratory
P.O. Box 451
Princeton, NJ 08543

Phone: 609-243-2245
Fax: 609-243-2751
e-mail: pppl_info@pppl.gov
Internet Address: http://www.pppl.gov